

Structures and Fragmentations of Small Silicon Oxide Clusters by *ab Initio* Calculations

W. C. Lu,[†] C. Z. Wang,^{*,†} V. Nguyen,^{†,‡} M. W. Schmidt,[‡] M. S. Gordon,[‡] and K. M. Ho[†]

Ames Laboratory U. S. Department of Energy and Department of Physics, Iowa State University, Ames, Iowa 50011 and Ames Laboratory U. S. Department of Energy and Department of Chemistry, Iowa State University, Ames, Iowa 50011

Received: December 30, 2002; In Final Form: May 14, 2003

The structures, energies, and fragmentation stabilities of silicon oxide clusters Si_mO_n , with $m = 1-5$, $n = 1, 2m + 1$, are studied systematically by *ab initio* calculations. New structures for nine clusters are found to be energetically more favorable than previously proposed structures. Using the ground state structures and energies obtained from our calculations, we have also studied fragmentation pathways and dissociation energies of the clusters. Our computational results show that the dissociation energy is strongly correlated with the O/Si ratio. Oxygen-rich clusters tend to have larger dissociation energies, as well as larger HOMO–LUMO gaps. Our calculations also show that SiO is the most abundant species in the fragmentation products.

I. Introduction

As the most abundant constituent on earth,¹ silicon oxide materials play a very important role in many areas of modern technology. Silicon and silicon dioxide, for example, are the heart and soul of the microelectronic industry. Silica glass is one of the key materials in optical fiber communications.^{2,3} Recently, silicon oxides have attracted great interest in the growth of nanosized materials. It was found in experiments that the growth of silicon nanowires will be greatly enhanced if silicon oxide is presented during the synthesis.⁴ This suggests that small silicon oxide clusters may have an important effect on the growth of nanosized materials.

The structure and properties of silicon oxide clusters has received considerable experimental^{5–11} as well as theoretical^{12–19} interest in the past decade. Knowledge about the structures and stabilities of clusters can be expected to provide useful information in elucidating microscopic aspects of condensed-phase phenomena.²⁰ Photoelectron spectra of a number of silicon oxide cluster anions including Si_3O_y^- ($y = 1-6$), Si_nO_n^- ($n = 3-5$), $(\text{SiO}_2)_n^-$ ($n = 1-4$), and $\text{Si}(\text{SiO}_2)_n^-$ ($n = 2, 3$) have been studied extensively by Wang et al.^{6–8} These experimental studies have provided useful information for the electronic structures of the clusters, but the information about the geometric structures is only indirect. Using first-principles density functional calculations, Chelikowsky and co-workers have studied the geometric structures and electronic properties of neutral and charged Si_nO_n ($n = 3, 4$, and 5) clusters.¹² Their computational results suggested that buckled rings are more stable than planar ones for Si_4O_4 and Si_5O_5 . The structures and properties of $(\text{SiO}_2)_n$ ($n = 1-6$) and Si_3O_n ($n = 1, 3, 4$) clusters have been studied by Nayak et al using *ab initio* calculations.¹⁵ They have shown that a double oxygen bridged motif is energetically favored for $(\text{SiO}_2)_n$ ($n = 2-6$) clusters. Recently, Chu et al. have performed a detailed computational study of the structures of Si_nO_m ($n, m = 1-8$) clusters using the DFT-B3LYP method and suggested several new geometries for these clusters.^{18,19}

Despite many efforts, our understanding of the structures and properties of silicon oxide clusters is still far from complete. In this paper, we present a systematic study on the structures and stabilities of SiO_n ($n = 1-4$), Si_2O_n ($n = 1-5$), Si_3O_n ($n = 1-7$), Si_4O_n ($n = 1-9$), and Si_5O_n ($n = 1-11$) clusters. From this systematic study, we obtained better structures for nine clusters in comparison with those published in the literature and new structures for four clusters that have not been studied. Using the structures and energies obtained from our systematic calculations, we have also studied the dissociation pathways and energies of the clusters. Such calculations provide useful insights into the stability of the clusters. This paper is arranged as follows: In section II, the computational methods are described. In section III, the low-energy structures of the clusters obtained from our calculations are presented. Dissociation behavior and relative stability of the clusters are discussed in section IV, followed by conclusions in section V.

II. Computational Methods

Global structure optimization is an outstanding challenge. Although simulated annealing using *ab initio* molecular dynamics (MD) or Monte Carlo (MC) could in principle be applied to search for the global minimum structures for clusters, such an approach is not efficient for systems that have strong chemical bonds and a bumpy potential energy landscape. This is the case for the Si–O systems studied in the present paper.²¹ The simulation time required to locate the global minimum of a silicon oxide cluster containing more than 10 atoms may well be beyond feasible computational limits. As far as we know, application of simulated annealing methods to silicon oxide clusters has been successful for only a few small clusters (e.g., Si_3O_3 and Si_4O_4).¹² In this paper, we will report a systematic study for Si_mO_n clusters with m ranging from 1 to 5 and n from 1 to $2m + 1$. Due to the limitation in the simulation time scale as mentioned above, simulated annealing using *ab initio* molecular dynamics for such a large number of clusters is not practical. We therefore utilize a structure optimization scheme based on human input and our knowledge of chemical bonding in silicon oxide clusters. We have carefully investigated more than 200 structures of different possible motifs by *ab initio*

* Corresponding author. Email: wangcz@ameslab.gov.

[†] Ames Laboratory U. S. Department of Energy and Department of Physics.

[‡] Ames Laboratory U. S. Department of Energy and Department of Chemistry.

TABLE 1: Comparison of Total Energies (in a.u.) Calculated at MP2/6-31G(d) and Single-Point MP2/6-31G(d) Using the DFT-B3LYP/6-31G(d) Geometries

	SiO	SiO ₂	Si ₂ O ₄	Si ₃ O ₄
MP2/6-31G(d)	-364.045974	-439.077378	-878.306798	-1167.414581
MP2/6-31G(d)//B3LYP/6-31G(d)	-364.045631	-439.077052	-878.306396	-1167.414300

calculations. Structure optimizations were performed by GAMESS code²² using density functional theory (DFT) with the B3LYP functional²³ and the 6-31G(d) basis set²⁴. The GAMESS code is a widely used approach that has been very successful for hundreds of molecules and clusters of the size investigated in the current work.

Once the optimized structures have been obtained for each cluster size, frequency analyses were performed for the lowest-energy isomers and for those isomers that have energies within 0.5 eV with respect to the corresponding lowest-energy ones, to ensure that these structures are indeed in local minima. We have also checked the spin states for several small silicon oxide clusters (SiO, SiO₂, Si₂O, Si₂O₂, and Si₃O₃) and found that the ground-states of all these clusters are singlets. We therefore assume singlet ground states for all larger silicon oxide clusters in the present calculations. However, the triplet spin states are used for Si, Si₂, Si₃, O, and O₂ atoms and molecules for determining the fragmentation pathways and dissociation energies as discussed in section IV.

The DFT method is used for the optimizations because a large number of structures are studied in this work. Higher level calculations for optimizing the structures of such a large number of clusters would be computationally very expensive. Nevertheless, after the structures are optimized by DFT, single point second-order perturbation theory (MP2)²⁵/6-31G(d) calculations are performed for all the lowest-energy structures using the coordinates obtained from the DFT-B3LYP optimizations. We have tested some structures by re-optimizing with MP2 and found that the optimized DFT-B3LYP coordinates are similar to those obtained by the MP2 optimizations. For example, the energies of SiO, SiO₂, Si₂O₄, and Si₃O₄ obtained from the single point MP2 calculations are very close to those obtained by MP2 optimizations, as one can see from the comparison in Table 1. Therefore, the single point MP2 calculations using the DFT structures should be very close to the fully optimized MP2 results.

III. Low-Energy Structures

The low-energy structures of the clusters obtained from our present calculations are plotted in Figures 1–5. Several isomers are plotted for each cluster size, for the purpose of comparison and discussion. Relative energies with respect to the corresponding lowest-energy isomers are also shown in the figures. In addition, binding energies of the lowest-energy structures from both DFT-B3LYP and the single point MP2 calculations are shown in Figure 6. The binding energies are defined with respect to Si atom and 1/2O₂. The binding energies as a function of cluster size from the DFT and MP2 calculations are in general very similar, although the MP2 binding energies are slightly larger than those from the DFT calculations, especially for oxygen-rich clusters. From this systematic study, we obtained new low-energy structures for nine clusters as compared to previous studies. These clusters include SiO₄, Si₃O₂, Si₄O, Si₄O₂, Si₅O₂, Si₅O₃, Si₅O₄, Si₅O₅, and Si₅O₇.

3.1. SiO_n. First, consider SiO_n ($n = 1-4$) clusters in which only one silicon atom is involved and the number of oxygen atoms ranges from 1 to 4. A set of lower-energy structures for these clusters are shown in Figure 1. Our calculations show

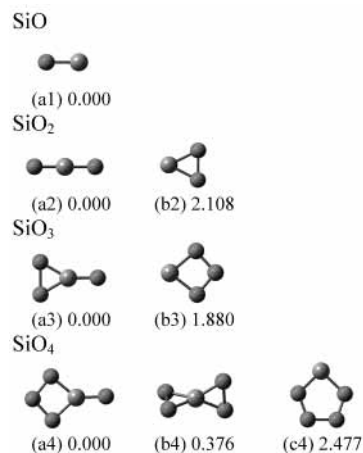


Figure 1. Low-energy isomers of SiO_n clusters. The darker balls are oxygen atoms. The numbers under the structures are relative energies (in eV) with respect to that of the corresponding lowest-energy isomers.

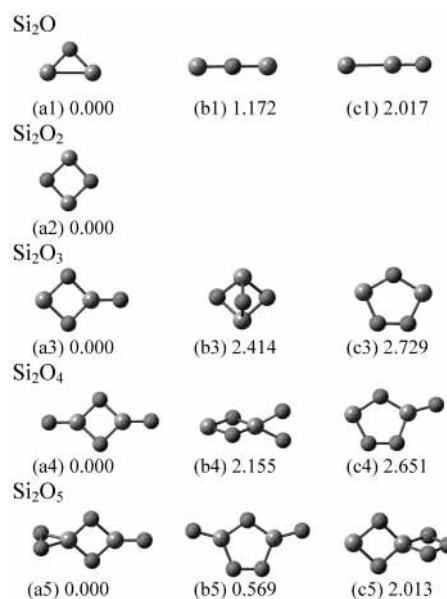


Figure 2. Lower-energy structures of Si₂O_n clusters. The darker balls are oxygen atoms. The numbers under the structures are relative energies (in eV) with respect to that of the corresponding lowest-energy isomers.

that SiO has a singlet ground state, in agreement with previous calculations.¹⁶ The binding energies (BE_n) of SiO with respect to Si and O atoms are calculated to be 7.738 eV at B3LYP/6-31G(d) and 7.913 eV at MP2/6-31G(d)//B3LYP/6-31G(d). In ref 16, the dissociation energy of SiO is calculated to be 7.892 eV (182.0 kcal/mol) using QCISD(T)/6-311+G(2df)//MP2(full)/6-311+G*. The current MP2 value is in good agreement with the previous QCISD(T) result and is 0.324 eV smaller than the experimental result of 8.237 eV (at $T = 0$ K).²⁶ For SiO₂, our calculations predict that the linear structure (Figure 1(a2)) is much more stable than the triangular structure (Figure 1(b2)). Several isomers have been considered for each of the two oxygen-rich clusters SiO₃ and SiO₄. The SiO₄ tetrahedral structure (Figure 1 (b4)) has previously been proposed in the literature as the ground-state structure.¹⁸ However, our results

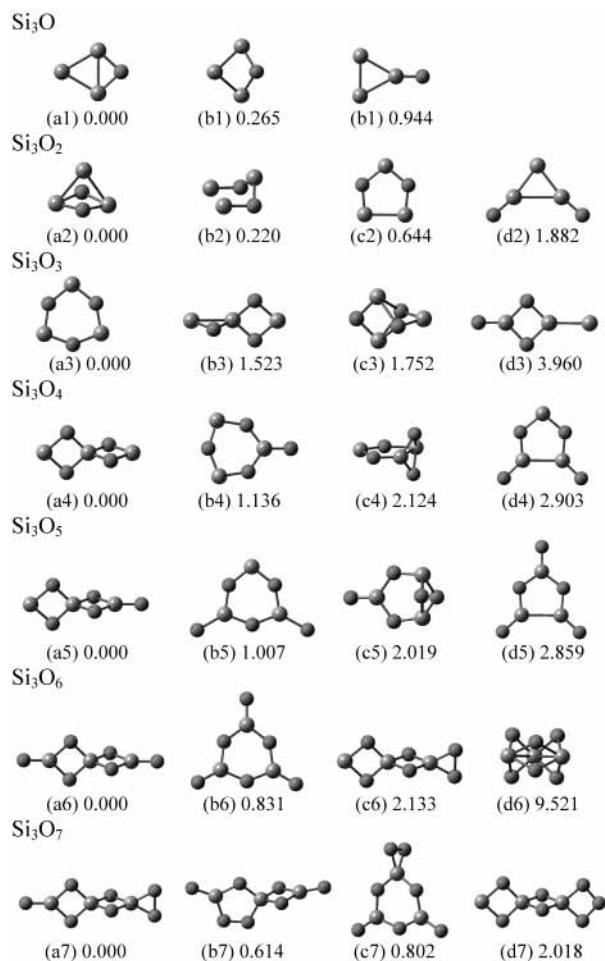


Figure 3. Lower-energy structures of Si_3O_n clusters. The darker balls are oxygen atoms. The numbers under the structures are relative energies (in eV) with respect to that of the corresponding lowest-energy isomers.

suggest that the lowest-energy structures of both SiO_3 and SiO_4 are the planar structures shown in Figure 1 (a3) and (a4). The DFT energy of planar SiO_4 is lower than that of the previously proposed tetrahedral SiO_4 by 0.376 eV.

3.2. Si_2O_n . As a prototype of small silicon clusters interacting with O atom, Si_2O has attracted both theoretical and experimental interest. It was predicted by Boldyrev and Simons¹⁶ that triangular Si_2O (singlet), shown in Figure 2 (a1), is the most stable structure. This structure was later confirmed by experiment.⁹ Our results show that the triangular Si_2O is indeed more stable than the linear SiOSi and SiSiO structures, in agreement with the above-mentioned theoretical and experimental results. When two O atoms are connected to two Si atoms (Si_2O_2), the lowest-energy structure is a rhombus as shown in Figure 2 (a2). This rhombus structure has been proposed both experimentally and theoretically.^{5,10,13} For Si_2O_3 , the structure with an O atom bonded to the Si_2O_2 -rhombus (Figure 2 (a3)) is energetically more favorable than the monocyclic structure (Figure 2 (c3)), suggesting that the O–O bond is not favorable in silicon oxide clusters. The Si_2O_4 cluster, which has an O/Si ratio of 2:1, favors a D_{2h} structure with a Si_2O_2 rhombus and two $\text{Si}=\text{O}$ double bonds on each side of the rhombus (Figure 2 (a4)). The structure in such a configuration is lower in energy than the structure with two O atoms bonded to the same Si atom of the Si_2O_2 rhombus (Figure 2 (b4)). The most stable structures of Si_2O_3 and Si_2O_4 clusters obtained from the present calculations are in good agreement with those suggested based on the experiments

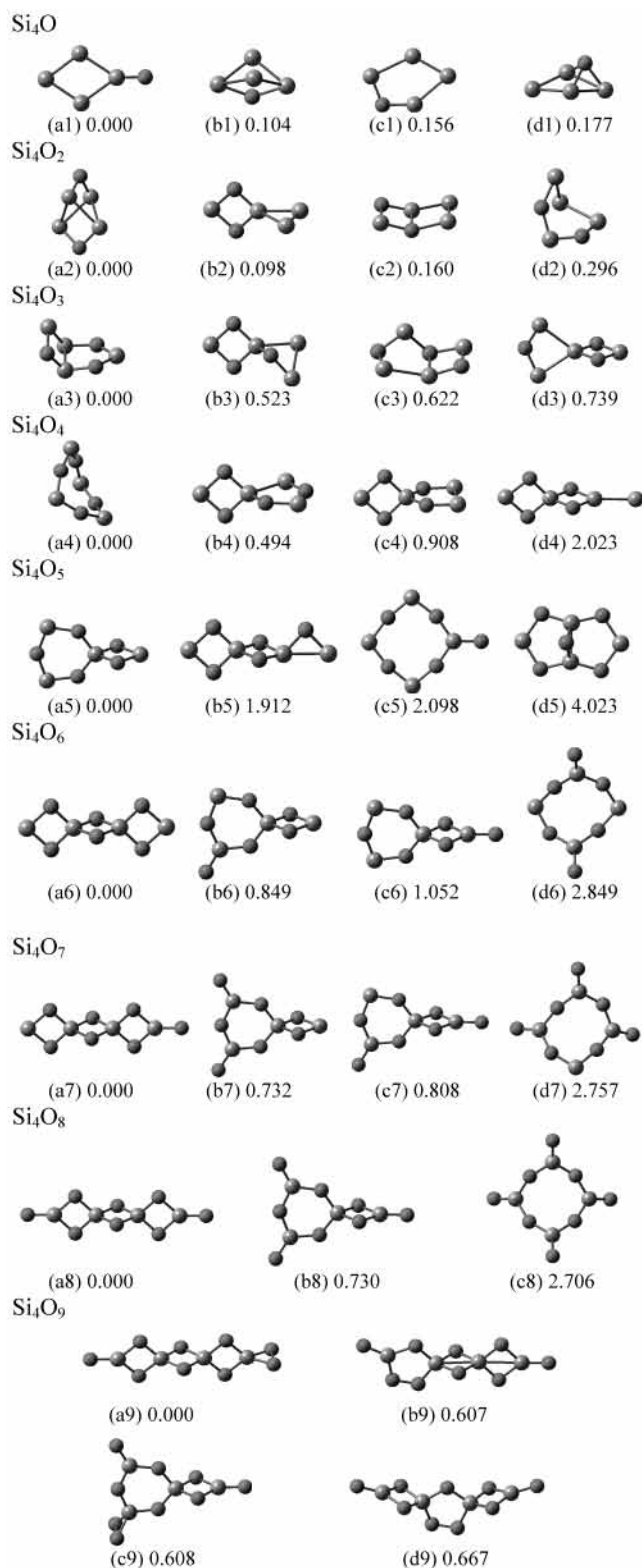


Figure 4. Lower-energy structures of Si_4O_n clusters. The darker balls are oxygen atoms. The numbers under the structures are relative energies (in eV) with respect to that of the corresponding lowest-energy isomers.

of Wang et al.⁸ When an additional O atom is attached to Si_2O_4 (i.e., Si_2O_5), the binding energy is only slightly larger than that of Si_2O_4 .

3.3. Si_3O_n . The low-energy structures of Si_3O_n clusters are plotted in Figure 3. For Si_3O , the lowest-energy structure is the one with an O atom bonded to two Si atoms of a Si_3 cluster. This structure is consistent with that predicted in refs 6, 15,

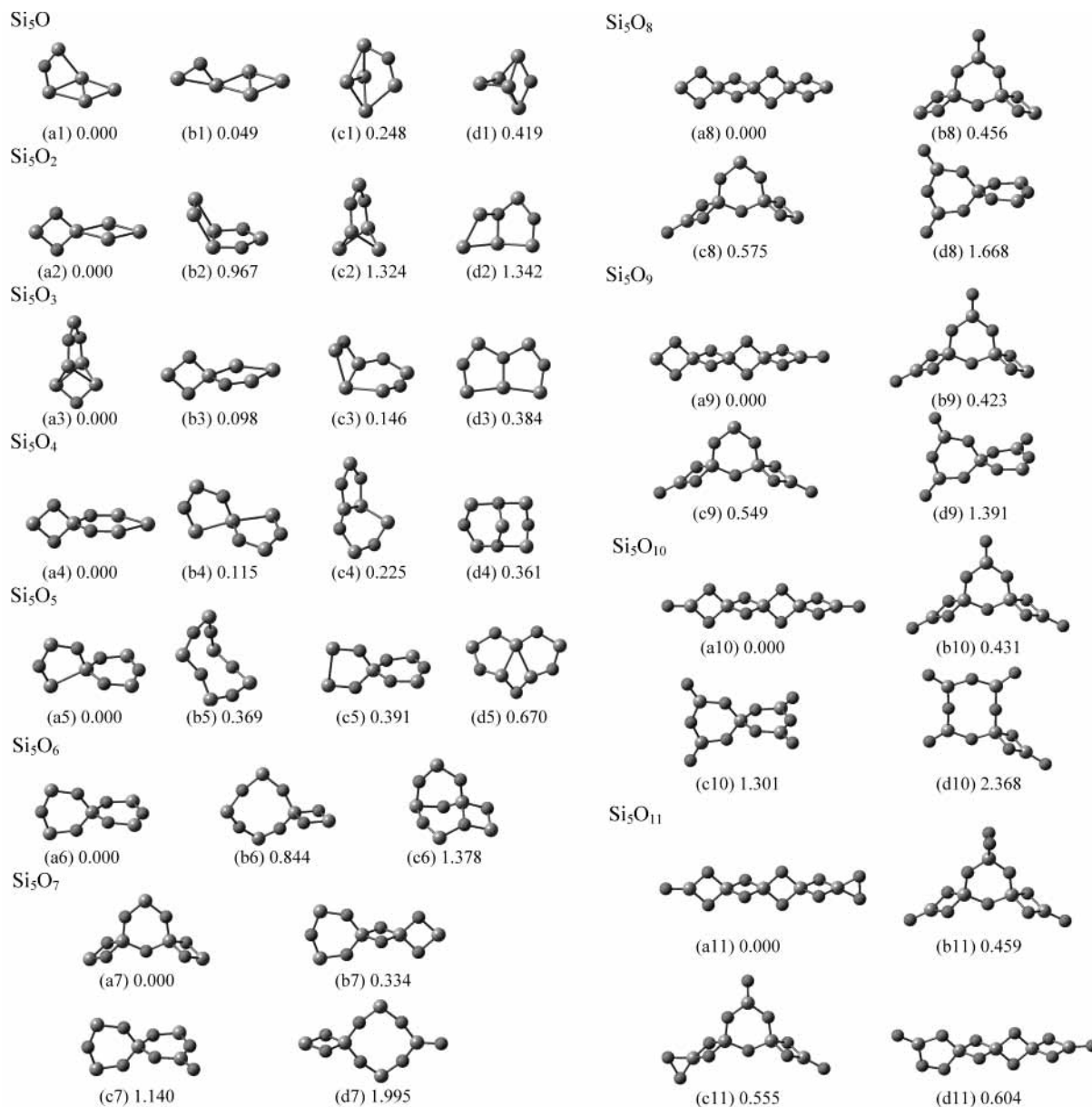


Figure 5. Lower-energy structures of Si_5O_n clusters. The darker balls are oxygen atoms. The numbers under the structures are relative energies (in eV) with respect to that of the corresponding lowest-energy isomers.

and 16. However, for Si_3O_2 , the previously predicted ring structure (Figure 3 (c2)) (ref 6) is found to be less stable than the structure (Figure 3 (a2)) obtained from the present calculations. Si_3O_3 has been studied extensively^{5,6,12} by both calculations and experiments. In the present study, the planar D_{3h} ring structure is shown to be the most stable isomer, consistent with previous studies. For Si_3O_4 , Si_3O_5 , and Si_3O_6 , the energetically favorable structures in each case are the double oxygen bridged chains with adjacent rhombuses oriented perpendicular to each other. Such double oxygen bridged structures have also been proposed by previous theoretical and experimental studies.^{6,15,18} Our calculations show clearly that the rhombus chain structures are more stable than ring structures for these clusters. Nayak and co-workers¹⁵ have ascribed the stability of rhombus chain structures to the preference of Si for 4-fold coordinated and O for 2-fold coordinated configurations. Finally, our calculations show that Si_3O_7 , with an additional O atom added to Si_3O_6 , is energetically unfavorable.

3.4. Si_4O_n . Low-energy structures of Si_4O_n clusters obtained from our calculations are plotted in Figure 4. Unlike those of

Si_2O and Si_3O , the lowest-energy structure of Si_4O is not a ring structure as suggested by ref 18. Rather, it is a structure with an O atom bonded directly to the lowest-energy structure of the Si_4 cluster (Figure 4 (a1)). We have studied 12 Si_4O_2 isomers and found that the lowest-energy isomer is a buckled Si_4 rhombus bridged by two O atoms from both top and bottom in a perpendicular orientation (see Figure 4 (a2)). This structure is more stable than the previously proposed ring structure as shown in Figure 4 (d2).¹⁸ Seven Si_4O_3 isomers were investigated. The lowest-energy structure is predicted to be the a ring-like structure shown in Figure 4 (a3), consistent with the computational results of Chu et al.¹⁸

The buckled ring structure of Si_4O_4 has been studied previously.^{7,12,18} In contrast to the planar Si_3O_3 ring structure, the predicted most stable Si_4O_4 isomer is a nonplanar buckled eight-membered ring structure, consistent with the computational prediction by Chelikowsky et al.¹² For Si_4O_5 , calculations have been performed for eight different isomers in order to find the lowest-energy structure. The predicted most favorable structure is a combination of a Si_3O_3 -ring and Si_2O_2 -rhombus as shown

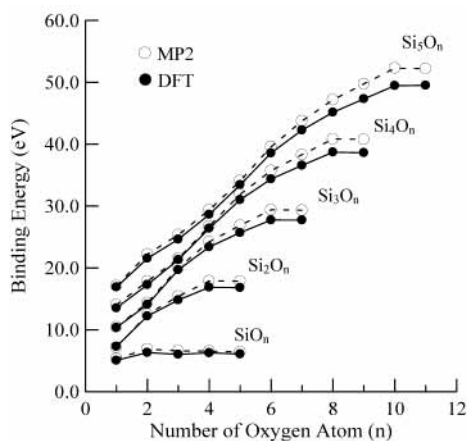


Figure 6. Binding energies of Si_mO_n clusters defined by $E(\text{Si}_m\text{O}_n) - mE(\text{Si}) - n/2E(\text{O}_2)$ from DFT-B3LYP/6-31G(d) and MP2/6-31G(d)//B3LYP/6-31G(d) calculations.

in Figure 4 (a5). This prediction is in agreement with the previous study of Chu et al.¹⁸ The dihedral angle formed by the Si_3O_3 ring and the Si_2O_2 ring is almost 90° . The other linear O-bridged structures and larger ring structures are less stable. For Si_4O_6 , Si_4O_7 , and Si_4O_8 , the lowest-energy structures are all rhombus chain structures with double oxygen bridges. This is consistent with previous computational results.^{15,18} For Si_4O_6 , we have also optimized a 3D cage structure, similar to that in ref 27; however, the Si_4O_6 cage was found to be much less stable with an energy of 5.425 eV higher than that of the lowest-energy structure. It is interesting to note that when the number of oxygen atoms in the cluster is more than twice the number of silicon atoms, the cluster is found to be less stable. For example, Si_4O_9 has a smaller binding energy than that of Si_4O_8 as one can see from Figure 6. Similarly, by the same measure, Si_2O_5 and Si_3O_7 are energetically less stable than Si_2O_4 and Si_3O_6 , respectively, as discussed in previous subsections.

3.5. Si_5O_n . While the lowest-energy structure of Si_4O corresponds to the one with an O atom bonded directly to the most stable Si_4 cluster, isomers that result from attaching an O atom to the most stable Si_5 cluster are not the most stable Si_5O isomers. As seen in Figure 5, the isomers (a1) and (b1) of Si_5O are very close in energy. Both structures are formed by addition of a SiO to the Si_4 rhombus. For Si_5O_2 , the lowest-energy structure is a combination of two rhombuses, the Si_2O_2 rhombus and a pure Si_4 rhombus as shown in Figure 5 (a2). This structure is the most stable among the 14 isomers investigated in the present work.

Si_5O_3 has been studied previously; the proposed structure in ref 18 corresponds to the isomer Si_5O_3 (d3) shown in Figure 5. In the present study, the most stable isomer of Si_5O_3 is predicted to have a bell-like structure shown in Figure 5 (a3). This structure has the same motif as the lowest-energy isomer of Si_4O_2 . The Si_5O_3 isomer can be formed by replacing the top O atom in Si_4O_2 with a SiO_2 unit. For Si_5O_4 , Si_5O_5 , and Si_5O_6 , the lowest-energy structures are all composed of two perpendicularly connected rings. It should be noted that Si_5O_5 is commonly believed to have a ring structure like the Si_2O_2 , Si_3O_3 , and Si_4O_4 clusters. However, in this study, it is found that a double ring structure (Figure 5 (a5)) is more stable than the single ring structure previously proposed. This suggests that larger ring structures are less stable and can decompose into smaller multi-rings units. For Si_5O_6 , the lowest-energy Si_5O_6 structure is found to be composed of two perpendicularly connected Si_3O_3 rings, in agreement with the predicted structure of ref 18. We also constructed a cage structure for Si_5O_6 .

However, the cage structure was found to be very unstable and transforms to the structure of two connected Si_4O_4 and Si_2O_2 rings (Figure 5 (b6)) after optimization. When an additional O atom is added, the most stable structure of Si_5O_7 corresponds to the three-ring structure as shown in Figure 5 (a7), in which two Si_2O_2 rhombuses are perpendicularly connected to the each side of the Si_3O_3 ring. This structure is more stable than the structure previously predicted (Figure 5 (b7)).¹⁸ For oxygen-rich Si_5O_8 , Si_5O_9 and Si_5O_{10} species, the most favorable structures are again all predicted to be double oxygen bridged chains. The structures of Si_5O_8 and Si_5O_{10} are consistent with computational results of Nayak et al. and Chu et al.^{15,18} Finally, the lowest-energy structure of Si_5O_{11} is shown to have a binding energy very close to that of Si_5O_{10} , once again indicating that the cluster with an O abundance that is more than twice of Si is less stable.

IV. Fragmentation Pathways and Dissociation Energies

Studies of fragmentation pathways and dissociation energies provide useful information for understanding the stability of the clusters. Such studies, for example, have been performed experimentally and theoretically for silicon clusters and have proven to be a very powerful method for analyzing the stability of the clusters.²⁸ It has been found that clusters that frequently appear in the fragmentation products are likely to be relatively stable clusters. Using the energies of the clusters obtained from the calculations discussed in section. III, we have investigated all possible fragmentation pathways and corresponding dissociation energies for the silicon oxide clusters studied in this work.

The dissociation energy for fragmentation pathway $\text{Si}_m\text{O}_n \rightarrow \text{Si}_k\text{O}_l + \text{Si}_{m-k}\text{O}_{n-l}$ is given by

$$DE_0 = E(\text{Si}_k\text{O}_l) + E(\text{Si}_{m-k}\text{O}_{n-l}) - E(\text{Si}_m\text{O}_n)$$

In the present calculation, the completely separated "atomic" products are assumed to be $n/2$ O_2 molecules (if n is even) or the energy of $(n-1)/2$ $\text{O}_2 + \text{O}$ atom (if n is odd). The energies of pure Si_m clusters are also used if the fragmentations separate the Si_mO_n clusters into pure silicon clusters and oxygen gas. The fragmentation pathways and dissociation energies have been analyzed using both DFT and MP2//DFT calculations. Zero-point vibration energies are also included in the DFT energies for the fragmentation calculations.

The low-energy fragmentation pathways and corresponding dissociation energies obtained from our analyses using DFT and MP2 energies are listed in Table 2 and Table 3, respectively. Only those pathways that are within ~ 0.7 eV of the lowest-energy fragmentation pathway are included in these tables. The fragmentation pathways from the DFT calculations are not affected by including the zero-point vibrational energies. The dissociation energies are shifted toward lower energies by less than a tenth of eV when the zero-point vibrational energies are included. The results from the MP2 calculations are similar to those of DFT, except for those clusters that have multiple fragmentation pathways that are within less than 1 eV in energy. For these clusters the competing fragmentation channels are the same for the two methods, but the relative dissociation energies among the channels are different for the two methods. For example, for the clusters with an O/Si ratio of 2 (i.e., Si_3O_6 , Si_4O_8 , and Si_5O_{10}), MP2 calculations tend to favor pathways that have SiO_2 as product, while DFT calculations prefer the fragmentation of an O_2 molecule. This difference can be partially attributed to the differences in the MP2 and DFT binding

TABLE 2: Total Energies (E_0 and E), Fragmentation Channels, Dissociation Energies (DE_0 and DE), and HOMO–LUMO Gaps (H–L Gap) of Si_mO_n Clusters from DFT- B3LYP/6-31G(d) Calculations

cluster	O/Si	E_0 (a.u.) ^a	E (a.u.) ^b	fragmentation channel	DE_0 (eV) ^c	DE (eV) ^d	H–L gap (eV)
SiO	1.00	−364.63501	−364.63220	Si + O	7.738	7.662	6.490
SiO ₂	2.00	−439.81146	−439.80488	SiO + O	3.953	3.850	5.673
SiO ₃	3.00	−514.93065	−514.92109	SiO + O ₂	0.967	0.885	5.344
Si ₂ O	0.50	−654.03679	−654.03242	SiO + Si	2.240	2.197	2.313
Si ₂ O ₂	1.00	−729.34749	−729.33887	SiO + SiO	2.108	2.026	4.111
Si ₂ O ₃	1.50	−804.57305	−804.55975	SiO + SiO ₂	3.444	3.338	5.600
Si ₂ O ₄	2.00	−879.77881	−879.76114	SiO ₂ + SiO ₂	4.242	4.120	5.730
				or Si ₂ O ₂ + O ₂	4.660	4.516	
				or Si ₂ O ₃ + O	4.750	4.631	
Si ₂ O ₅	2.50	−954.90688	−954.88586	Si ₂ O ₃ + O ₂	2.006	1.900	5.284
				or Si ₂ O ₄ + O	2.636	2.544	
Si ₃ O	0.33	−943.46883	−943.46270	SiO + Si ₂	2.387	2.330	2.196
				Si ₂ O + Si	3.063	3.016	
Si ₃ O ₂	0.67	−1018.73526	−1018.72620	SiO + Si ₂ O	1.726	1.676	3.965
				or Si ₂ O ₂ + Si	1.858	1.847	
Si ₃ O ₃	1.00	−1094.07180	−1094.05841	SiO + Si ₂ O ₂	2.431	2.378	4.609
Si ₃ O ₄	1.33	−1169.33782	−1169.31798	SiO + Si ₂ O ₃	3.531	3.431	5.434
Si ₃ O ₅	1.67	−1244.55241	−1244.52834	SiO + Si ₂ O ₄	3.770	3.674	5.750
Si ₃ O ₆	2.00	−1319.75782	−1319.72946	Si ₃ O ₄ + O ₂	4.351	4.222	6.087
				or SiO ₂ + Si ₂ O ₄	4.557	4.448	
				or Si ₃ O ₅ + O	4.743	4.627	
Si ₃ O ₇	2.33	−1394.88748	−1394.85486	Si ₃ O ₅ + O ₂	2.039	1.910	5.281
				or Si ₃ O ₆ + O	2.681	2.564	
Si ₄ O	0.25	−1232.90428	−1232.89628	SiO + Si ₃	1.707	1.634	3.692
Si ₄ O ₂	0.50	−1308.17277	−1308.16097	SiO + Si ₃ O	1.877	2.116	2.403
				or Si ₂ O ₂ + Si ₂	2.156	2.421	
Si ₄ O ₃	0.75	−1383.45116	−1383.43580	Si ₃ O ₃ + Si	1.631	1.574	2.604
				or Si ₂ O ₂ + Si ₂ O	1.820	1.754	
				or SiO + Si ₃ O ₂	2.202	2.106	
Si ₄ O ₄	1.00	−1458.76782	−1458.74970	SiO + Si ₃ O ₃	1.661	1.608	3.924
				or Si ₂ O ₂ + Si ₂ O ₂	1.983	1.960	
Si ₄ O ₅	1.25	−1534.06763	−1534.04231	SiO + Si ₃ O ₄	2.581	2.508	4.667
Si ₄ O ₆	1.50	−1609.32100	−1609.28875	SiO + Si ₃ O ₅	3.637	3.488	5.619
Si ₄ O ₇	1.75	−1684.53186	−1684.49532	SiO + Si ₃ O ₆	3.783	3.637	5.747
Si ₄ O ₈	2.00	−1759.74025	−1759.69948	Si ₄ O ₆ + O ₂	4.328	4.202	6.179
				or SiO ₂ + Si ₃ O ₆	4.650	4.491	
				or Si ₄ O ₇ + O	4.823	4.707	
				or Si ₂ O ₄ + Si ₂ O ₄	4.969	4.820	
Si ₄ O ₉	2.25	−1834.86712	−1834.82315	Si ₄ O ₇ + O ₂	2.043	1.943	5.276
				or Si ₄ O ₈ + O	2.604	2.518	
Si ₅ O	0.20	−1522.34806	−1522.33884	SiO + Si ₄	0.937	0.890	2.168
Si ₅ O ₂	0.40	−1597.64886	−1597.63387	Si ₂ O ₂ + Si ₃	2.581	2.475	3.937
				or SiO + Si ₄ O	2.979	2.870	
Si ₅ O ₃	0.60	−1672.89250	−1672.87567	Si ₃ O ₃ + Si ₂	2.030	1.966	2.718
				or Si ₂ O ₂ + Si ₃ O	2.073	2.016	
				or SiO + Si ₄ O ₂	2.305	2.242	
Si ₅ O ₄	0.80	−1748.16946	−1748.14629	Si ₃ O ₃ + Si ₂ O	1.654	1.508	2.941
				or Si ₄ O ₄ + Si	2.235	2.096	
				or SiO + Si ₄ O ₃	2.265	2.129	
				or Si ₂ O ₂ + Si ₃ O ₂	2.358	2.209	
				or Si ₃ O ₄ + Si ₂	2.328	2.269	
Si ₅ O ₅	1.00	−1823.47629	−1823.45147	Si ₂ O ₂ + Si ₃ O ₃	1.555	1.471	3.064
				or Si ₄ O ₄ + SiO	2.000	1.890	
Si ₅ O ₆	1.20	−1898.79481	−1898.76543	SiO + Si ₄ O ₅	2.508	2.471	4.572
				or Si ₂ O ₂ + Si ₃ O ₄	2.979	2.953	
Si ₅ O ₇	1.40	−1974.06116	−1974.02394	SiO + Si ₄ O ₆	2.860	2.803	5.437
Si ₅ O ₈	1.60	−2049.29661	−2049.25478	SiO + Si ₄ O ₇	3.528	3.468	5.717
Si ₅ O ₉	1.80	−2124.50661	−2124.46105	SiO + Si ₄ O ₈	3.574	3.521	5.755
Si ₅ O ₁₀	2.00	−2199.71508	−2199.66486	Si ₅ O ₈ + O ₂	4.311	4.179	6.261
				or SiO ₂ + Si ₄ O ₈	4.444	4.365	
				or Si ₅ O ₉ + O	4.823	4.697	
				or Si ₂ O ₄ + Si ₃ O ₆	4.856	4.737	
Si ₅ O ₁₁	2.20	−2274.84697	−2274.79141	Si ₅ O ₉ + O ₂	2.186	2.020	5.287
				or Si ₅ O ₁₀ + O	2.737	2.597	

^a Total energies (E_0) without zero-point corrections. ^b Total energies (E) including zero-point corrections. ^c Dissociation energies (DE_0) without zero-point corrections. ^d Dissociation energies (DE) including zero-point corrections.

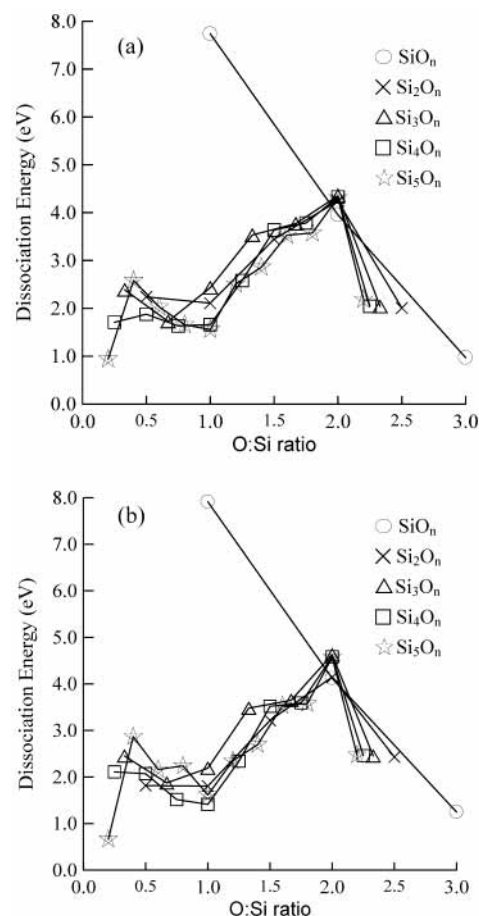
energies of O₂ and SiO₂ molecules. The DFT binding energy for O₂ is 5.381 eV, compared with the MP2 and experimental values of 5.161 and 5.120 eV, respectively. So, DFT significantly over-binds O₂, whereas MP2 is in reasonable agreement

with experiment. The DFT binding energy for SiO₂ is 6.310 eV, compared with the MP2 and experimental values of 6.871 and 6.769 eV, respectively. So in this case, DFT seriously under-binds SiO₂, while MP2 is again in good agreement with

TABLE 3: Total Energies (E_0), Fragmentation Channels, and Dissociation Energies (DE_0) of Si_mO_n Clusters from MP2/6-31G(d)//B3LYP/6-31G(d) Calculations

cluster	O/Si	E_0 (a.u.)	fragmentation channel	DE_0 (eV)
SiO	1.00	-364.04563	Si + O	7.913
SiO ₂	2.00	-439.07705	SiO + O	4.120
SiO ₃	3.00	-514.04111	SiO + O ₂	1.246
Si ₂ O	0.50	-652.98709	SiO + Si	1.814
Si ₂ O ₂	1.00	-728.15750	SiO + SiO	1.804
Si ₂ O ₃	1.50	-803.24082	SiO + SiO ₂	3.215
Si ₂ O ₄	2.00	-878.30640	SiO ₂ + SiO ₂	4.144
Si ₂ O ₅	2.50	-953.27978	Si ₂ O ₃ + O ₂	2.428
			or Si ₂ O ₄ + O	2.541
Si ₃ O	0.33	-941.98301	SiO + Si ₂	2.451
			Si ₂ O + Si	3.298
Si ₃ O ₂	0.67	-1017.10150	SiO + Si ₂ O	1.872
			or Si ₂ O ₂ + Si	1.882
Si ₃ O ₃	1.00	-1092.28359	SiO + Si ₂ O ₂	2.189
Si ₃ O ₄	1.33	-1167.41430	SiO + Si ₂ O ₃	3.478
Si ₃ O ₅	1.67	-1242.48612	SiO + Si ₂ O ₄	3.647
Si ₃ O ₆	2.00	-1317.55351	SiO ₂ + Si ₂ O ₄	4.627
			or Si ₃ O ₅ + O	5.099
			or Si ₃ O ₄ + O ₂	5.155
Si ₃ O ₇	2.33	-1392.52593	Si ₃ O ₅ + O ₂	2.451
			or Si ₃ O ₆ + O	2.514
Si ₄ O	0.25	-1230.98911	SiO + Si ₃	2.109
Si ₄ O ₂	0.50	-1306.10478	SiO + Si ₃ O	2.069
			or Si ₂ O ₂ + Si ₂	2.717
Si ₄ O ₃	0.75	-1381.21396	Si ₃ O ₃ + Si	1.515
			or SiO + Si ₃ O ₂	1.820
			or Si ₂ O ₂ + Si ₂ O	1.890
Si ₄ O ₄	1.00	-1456.38116	SiO + Si ₃ O ₃	1.412
			or Si ₂ O ₂ + Si ₂ O ₂	1.800
Si ₄ O ₅	1.25	-1531.54594	SiO + Si ₃ O ₄	2.338
Si ₄ O ₆	1.50	-1606.66101	SiO + Si ₃ O ₅	3.518
Si ₄ O ₇	1.75	-1681.73107	SiO + Si ₃ O ₆	3.591
Si ₄ O ₈	2.00	-1756.79891	SiO ₂ + Si ₃ O ₆	4.584
			or Si ₂ O ₄ + Si ₂ O ₄	5.065
			or Si ₄ O ₇ + O	5.112
			Si ₄ O ₆ + O ₂	5.122
Si ₄ O ₉	2.25	-1831.77117	Si ₄ O ₇ + O ₂	2.458
			or Si ₄ O ₈ + O	2.508
Si ₅ O	0.20	-1519.97759	SiO + Si ₄	0.661
Si ₅ O ₂	0.40	-1595.14012	SiO + Si ₄ O	2.867
			or Si ₂ O ₂ + Si ₃	3.175
Si ₅ O ₃	0.60	-1670.22971	SiO + Si ₄ O ₂	2.159
			or Si ₂ O ₂ + Si ₃ O	2.425
			or Si ₃ O ₃ + Si ₂	2.690
Si ₅ O ₄	0.80	-1745.35285	Si ₃ O ₃ + Si ₂ O	2.239
			or Si ₃ O ₄ + Si ₂	2.485
			or SiO + Si ₄ O ₃	2.538
			or Si ₄ O ₄ + Si	2.641
Si ₅ O ₅	1.00	-1820.50051	Si ₂ O ₂ + Si ₃ O ₃	1.614
			or Si ₄ O ₄ + SiO	2.006
			or Si ₄ O ₅ + Si	2.172
Si ₅ O ₆	1.20	-1895.67770	SiO + Si ₄ O ₅	2.345
			or Si ₂ O ₂ + Si ₃ O ₄	2.883
Si ₅ O ₇	1.40	-1970.80567	SiO + Si ₄ O ₆	2.694
Si ₅ O ₈	1.60	-2045.90645	SiO + Si ₄ O ₇	3.531
Si ₅ O ₉	1.80	-2120.97591	SiO + Si ₄ O ₈	3.574
Si ₅ O ₁₀	2.00	-2196.04402	SiO ₂ + Si ₄ O ₈	4.570
			or Si ₂ O ₄ + Si ₃ O ₆	5.009
			or Si ₅ O ₈ + O ₂	5.109
			or Si ₅ O ₉ + O	5.115
Si ₅ O ₁₁	2.20	-2271.01629	Si ₅ O ₉ + O ₂	2.471
			or Si ₅ O ₁₀ + O	2.511

experiment. (The experimental values are extrapolated to $T = 0$ K.²⁶) Similarly, the binding energy difference for SiO from DFT (7.738 eV) and MP2 (7.913 eV) may be used to explain why the SiO fragmentation channel is slightly favored in the MP2 calculation (e.g., for Si₄O₃, Si₅O₂, and Si₅O₃). Experimental data for the binding energies of SiO is 8.237 eV (extrapolate to $T = 0$ K).²⁶ Both DFT and MP2 energies are smaller than the

**Figure 7.** Dissociation energies of Si_mO_n clusters as a function of O/Si ratio from (a) DFT- B3LYP/6-31G(d) and (b) MP2/6-31G(d)//B3LYP/6-31G(d) calculations.

experimental value, although the MP2 result is closer to the experimental data.

The results in Tables 2 and 3 illustrate that (with some exceptions such as Si₂O₄, Si₃O₆, Si₄O₈, and Si₅O₁₀) the SiO molecule is the most abundant species in the fragmentation products of the clusters. The abundance of SiO in the gas phase of silicon oxide materials has been known for some time.^{29,30} It has been shown that solid SiO₂ in the presence of silicon vaporizes to SiO gas and that SiO₂ under neutral oxidizing conditions vaporizes by decomposition to gaseous SiO and oxygen. The present computational results are therefore consistent with the experimental observations. Besides SiO, production of Si₂O₂ and Si₃O₃ appear to be more frequent than other Si₂O_n and Si₃O_n clusters, suggesting that Si₂O₂ and Si₃O₃ may be relatively more stable species in the gas phase. Information about the abundance of Si₄O_n and Si₅O_n fragments would require the fragmentation of larger Si_mO_n clusters which is beyond the scope of the present study.

To determine if there is any correlation between the dissociation energies and the compositions of the clusters, we plot in Figure 7 the lowest dissociation energy as a function of the O/Si ratio for all clusters considered in this study. The figure shows that all Si_mO_{2m} clusters with an O/Si ratio of 2 have large dissociation energies of more than 4 eV. In general, the dissociation energies of the oxygen-rich clusters are larger than those of the silicon-rich clusters with a few exceptions. These exceptions are: (i) When the O:Si ratio is more than 2, the dissociation energy drops sharply, (ii) Although SiO has O/Si = 1, it has the highest dissociation energy of 7.738 (B3LYP) and 7.913 eV (MP2/6-31G(d)//B3LYP/6-31G(d)). The large

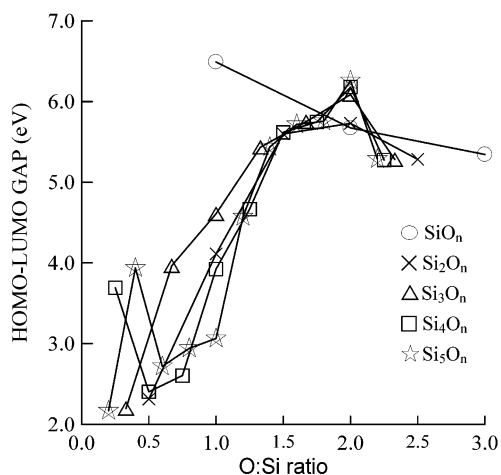


Figure 8. HOMO–LUMO gaps of Si_mO_n clusters as a function of O/Si ratio from DFT- B3LYP/6-31G(d) calculations.

dissociation energy of SiO can be attributed to the fact that the energies of Si and O atoms are much higher as compared to that of the SiO molecule, and that SiO formally has a triple bond (cf., its valence isoelectronic analogue CO). It is therefore energetically very unfavorable to break SiO into individual Si and O atoms. Figure 7 also shows that the dissociation energies of the Si_mO_n clusters have a minimum at stoichiometric or slightly oxygen-poor compositions. A transition from low dissociation energy to high dissociation energy seems to occur at an O/Si ratio between 1 and 1.5. It can be seen from Figure 7 that there is a big increase in dissociation energy between Si_2O_2 and Si_2O_3 in the Si_2O_n clusters, and between Si_3O_3 and Si_3O_4 in the Si_3O_n clusters. For the Si_4O_n and Si_5O_n clusters, a large energy increment also occurs between Si_4O_4 – Si_4O_5 and Si_5O_5 – Si_5O_6 , respectively.

Finally, we also plot the HOMO–LUMO gaps of the clusters as a function of the O/Si ratio in Figure 8. The behavior of the HOMO–LUMO gap with respect to the O/Si ratio is similar to that of the dissociation energy. In particular, clusters with an O/Si ratio of 2 are found to have the largest HOMO–LUMO gap (except that of SiO_2). This is understandable because all bonds in these clusters are saturated. The plot also shows that the HOMO–LUMO gaps of the oxygen-rich clusters are in general larger than those of the silicon-rich clusters, and the transition from small gap to large gap also occurs roughly at an O/Si ratio between 1 and 1.5.

V. Conclusions

In this work, we have performed a systematic study of SiO_n , Si_2O_n , Si_3O_n , Si_4O_n , and Si_5O_n clusters. We have obtained new structures for nine clusters which are energetically more stable than the structures proposed in the literature. We have also predicted the lowest-energy structures for four clusters that have not been studied before. On the basis of the structures and energies from our systematic calculations, we have analyzed the fragmentation pathways and the corresponding dissociation energies in great detail. We show that there is a strong correlation between the O/Si ratio and dissociation energy. The 1:2 ratio Si_nO_{2n} clusters tend to have the largest dissociation energies. The dissociation energies are also correlated with the HOMO–LUMO gaps of the clusters. Clusters with large

HOMO–LUMO gaps seem also to have large dissociation energies. Our results on the fragmentation pathways also provide useful information for understanding the relative stability of the clusters.

Acknowledgment. We would like to thank Tzu-Liang Chan for performing ab initio molecular dynamics simulations to check the stability of some structures from our calculations. Ames Laboratory is operated for the U.S. Department of Energy by Iowa State University under Contract No. W-7405-Eng-82. This work was supported by the Director for Energy Research, Office of Basic Energy Sciences including a grant of computer time at the National Energy Research Supercomputing Center (NERSC) in Berkeley. This work is also supported by Research Grant Council of Hong Kong under the RGC/CERG project No.9040533.

References and Notes

- (1) Holmes, D. L. *Elements of Physical Geology*; Ronald Press: New York, 1969.
- (2) Morey, G. W. *The Properties of Glass*, 2nd ed.; Reinhold: New York, 1954.
- (3) Desurvire, E. *Phys. Today* **1994**, *47*, 20.
- (4) Wang, N.; Tang, Y. H.; Zhang, Y. F.; Lee, C. S.; Lee, S. T. *Phys. Rev. B*, **1998**, *58*, R16024.
- (5) Anderson, J. S.; Ogden, J. S. *J. Chem. Phys.* **1969**, *51*, 4189.
- (6) Wang, L. S.; Nicholas, J. B.; Dupuis, M.; Wu, H.; Colson, S. D. *Phys. Rev. Lett.* **1997**, *78*, 4450.
- (7) Wang, L. S.; Desai, S. R.; Wu, H.; Nicholas, J. B. *Z. Phys. D* **1997**, *40*, 36.
- (8) Wang, L. S.; Wu, H.; Desai, S. R.; Fan, J.; Colson, S. D. *J. Phys. Chem.* **1996**, *100*, 8697.
- (9) Iraqi, M.; Goldberg, N.; Schwarz, H. *J. Phys. Chem.* **1993**, *97*, 11371.
- (10) Goldberg, N.; Iraqi, M.; Koch, W.; Schaltz, H. *Chem. Phys. Lett.* **1994**, *225*, 404.
- (11) Lafargue, P. E.; Gaumet, J. J.; Muller, J. F., *J. Mass Spectrom.* **1996**, *31*, 623.
- (12) Chelikowsky, J. R. *Phys. Rev. B* **1998**, *57*, 3333.
- (13) Snyder, L. C.; Raghavachari, K. *J. Chem. Phys.* **1984**, *80*, 5076.
- (14) Harkless, J. A. W.; Stillinger, D. K.; Stillinger, F. H. *J. Phys. Chem.* **1996**, *100*, 1098.
- (15) Nayak, S. K.; Rao, B. K.; Khanna, S. N.; Jena, P. *J. Chem. Phys.* **1998**, *109*, 1245.
- (16) Boldyrev, A. I.; Simons, J. *J. Phys. Chem.* **1993**, *97*, 5875.
- (17) Sommerfeld, T.; Scheller, M. K.; Cederbaum, L. S. *J. Chem. Phys.* **1995**, *103*, 1057; **1996**, *104*, 1464.
- (18) Chu, T. S.; Zhang, R. Q.; Cheung, J. F. *J. Phys. Chem. B* **2001**, *105*, 1705.
- (19) Zhang, R. Q.; Chu, T. S.; Cheung, H. F.; Wang, N.; Lee, S. T. *Phys. Rev. B* **2001**, *64*, 113304.
- (20) Castleman, A. W., Jr.; Bowen, K. H., Jr. *J. Phys. Chem.* **1996**, *100*, 12911.
- (21) We have performed simulated annealing using ab initio molecular dynamics to search for the ground-state structures of Si_4O , Si_4O_2 , and Si_5O_7 . However, we find no structures that are lower in energy than those discussed in this paper.
- (22) Schmidt, M. W.; Baldrige, K. K.; Boatz, J. A.; Elbert, S. T.; Gordon, M. S.; Jensen, J. H.; Koseki, S.; Matsunaga, N.; Nguyen, K. A.; Su, S. J.; Windus, T. L.; Dupuis, M.; Montgomery, J. A. *J. Comput. Chem.* **1993**, *14*, 1347.
- (23) Becke, A. D. *J. Chem. Phys.* **1993**, *98*, 5648.
- (24) Hariharan, P. C.; Pople, J. A. *Theor. Chim. Acta* **1973**, *28*, 213.
- (25) Head-Gordon, M.; Pople, J. A.; Frisch, M. J. *Chem. Phys. Lett.* **1988**, *153*, 503.
- (26) *J. Phys. Chem. Ref. Data*, Monograph No. 9, *NIST-HANAF Thermochemical Tables*, 4th edition, edited by M. W. Chase, Jr., 1998.
- (27) Xu, C.; Wang, W.; Zhang, W.; Zhuang, J.; Liu, L.; Kong, L.; Zhao, Y.; Long, K. Fan, S.; Qian, Y.; Li, J. *J. Phys. Chem. A* **2000**, *104*, 9518.
- (28) Raghavachari, K.; Rohlfing, C. M. *Chem. Phys. Lett.* **1988**, *143*, 428.
- (29) Brewer, L.; Edwards, R. K. *J. Phys. Chem.* **1954**, *58*, 351.
- (30) Porter, R. F.; Chupka, W. A.; Inghram, M. G. *J. Chem. Phys.* **1955**, *23*, 216.